

MIT Open Access Articles

Smooth muscle cells orchestrate the endothelial cell response to flow and injury

The MIT Faculty has made this article openly available. **Please share** how this access benefits you. Your story matters.

Citation: Balcells, M. et al. "Smooth Muscle Cells Orchestrate the Endothelial Cell Response to Flow and Injury." *Circulation* 121.20 (2010): 2192–2199. Web.

As Published: <http://dx.doi.org/10.1161/CIRCULATIONAHA.109.877282>

Publisher: American Heart Association

Persistent URL: <http://hdl.handle.net/1721.1/75728>

Version: Author's final manuscript: final author's manuscript post peer review, without publisher's formatting or copy editing

Terms of use: Creative Commons Attribution-Noncommercial-Share Alike 3.0





Published in final edited form as:

Circulation. 2010 May 25; 121(20): 2192–2199. doi:10.1161/CIRCULATIONAHA.109.877282.

Smooth muscle cells orchestrate the endothelial cell response to flow and injury

Mercedes Balcells, PhD^{1,2,*}, Jordi Martorell, MS^{1,2}, Carla Olive, MS^{1,2}, Marina Santacana, MS^{1,2}, Vipul Chitalia, MD, PhD^{1,3}, Angelo A. Cardoso, MD, PhD⁴, and Elazer R. Edelman, MD, PhD, FACC^{1,5}

¹ Harvard-MIT Division of Health Sciences and Technology, 77 Massachusetts Avenue, Cambridge, MA 02139

² Institut Químic de Sarrià, Ramon Llull University, Via Augusta 390, Barcelona 08017, Spain

³ Boston University School of Medicine, 85 E Concord St, Boston, MA 02118

⁴ Indiana University School of Medicine and Simon Cancer Center, 980W. Walnut Street, Indianapolis, IN 46202

⁵ Cardiovascular Division, Brigham and Women's Hospital and Harvard Medical School, 75 Francis Street, Boston, MA 02115

Abstract

Background—Local modulation of vascular mTOR signaling reduces smooth muscle cells (SMC) proliferation after endovascular interventions but may be associated with endothelial cell (EC) toxicity. The trilaminar vascular architecture juxtaposes EC and SMC to enable complex paracrine co-regulation, but shields SMC from flow. We hypothesized that flow differentially impacts mTOR signaling in EC and SMC, and that SMC regulate mTOR in EC.

Methods and Results—SMC and/or EC were exposed to coronary artery flow in a perfusion bioreactor. We demonstrated by flowcytometry, immunofluorescence and immunoblotting that EC expression of phospho-S6 ribosomal protein (p-S6RP), a downstream target of mTOR, was doubled by flow. Conversely, S6RP in SMC was growth factor-, but not flow-, responsive and SMC eliminated the flow-sensitivity of EC. Temsirolimus, a sirolimus analog, eliminated the effect of GF on SMC and flow on EC, reducing p-S6RP below basal levels and inhibiting endothelial recovery. EC p-S6RP expression in stented porcine arteries confirmed our in vitro findings – phosphorylation was greatest in EC farthest from intact SMC in metal stented arteries and altogether absent after sirolimus stent-elution.

Conclusions—mTOR pathway is activated in EC in response to luminal flow. SMC inhibit this flow-induced stimulation of endothelial mTOR pathway. Thus, we now define a novel external stimulus regulating phosphorylation of S6RP and another level of EC-SMC cross-talk. These interactions may explain the impact of local anti-proliferative delivery that targets SMC proliferation, and suggest that future stents integrate design influences on flow and drug effects on their molecular targets.

*To whom correspondence and proofs should be addressed. MIT, 77 Massachusetts Avenue, Cambridge, MA 02139. merche@mit.edu, Tel.: (617) 324 0054, FAX: (617) 253 2514.

Clinical Trial Registration Information: N/A

CONFLICT OF INTEREST DISCLOSURES

None

Keywords

Blood flow; endothelium; muscle smooth; stents; molecular biology

INTRODUCTION

Local delivery of anti-proliferative drugs limits the intimal hyperplastic response to vascular intervention, but may place vessels at risk of thrombosis even late after initial treatment. The intervention, agents used and means of administration can synergistically induce endothelial dysfunction and delay recovery¹ leading to impaired vasoreactivity, enhanced platelet aggregation², and elevated tissue factor expression^{3, 4, 5}. Sirolimus, for example, inhibits smooth muscle cell (SMC) proliferation and intimal hyperplasia after vascular manipulation presumably through effects on signaling within the mammalian target of rapamycin (mTOR) pathway. mTOR is central to regulation of protein synthesis, ribosomal protein translation, and cap-dependent translation⁶, and its inhibition with sirolimus alters the balance of mTORC1 - mTORC2 complexes⁷. Prolonged exposure to sirolimus partially inhibits Akt activation and smooth muscle cell proliferation⁸. But sirolimus also induces tissue factor expression^{3, 4} and dysfunction in endothelial cells (EC). The impact of flow and drug release on tissue drug distribution and vascular repair has been defined computationally⁹⁻¹² and *in vivo*¹³⁻¹⁵ but the specific flow effects on individual vascular cells has not been fully defined. EC are especially flow-sensitive¹⁶ and altered hemodynamics may disrupt endothelial health. When EC become dysfunctional, vascular homeostasis is disrupted and disease becomes manifest -each element of vascular repair goes awry¹⁷.

We used vessel-like constructs to examine mTOR-pathway signaling in isolated EC, isolated SMC and EC cultured over SMC. A model system with sequentially layered SMC/EC vessel-like constructs connected to a perfusion bioreactor allowed for fine control of hemodynamic parameters, recapitulating physiologic flow. Importantly, these constructs enabled biologically-relevant studies of vascular intervention, including bolus drug administration, balloon deployment and stent implantation. Our data demonstrate a profound difference in EC biology in the presence and absence of SMC and suggests a far more sophisticated regulatory interaction between alterations in hemodynamics from above and vessel wall from below than classically appreciated.

MATERIALS AND METHODS

Vascular cell culture and bioengineered vessel-like construct

Human coronary artery endothelial cells (EC) (Promocell) were cultured in EBM-2 basal medium (Lonza) supplemented with 5% FBS, 1% penicillin-streptomycin, 0.04% hydrocortisone, 0.4% human-FGF-2, 0.1% VEGF, 0.1% R3-IGF-1, 0.1% ascorbic acid, 0.1% human-EGF, and 0.1% gentamicin-amphotericin 1000 (EC complete medium). Human aortic smooth muscle cells (SMC, Cambrex) were cultured with SmBM-2 basal medium (Lonza) supplemented with 5% CS, 1% glutamine, and 1% penicillin-streptomycin (SMC complete medium). Cells, passage 4-6, were fed every 48h, and incubated at 37°C.

Prior to cell seeding, 3.18mm ID Silastic® tubes (Dow Corning) were washed in 0.2% SDS for 20min, rinsed twice with distilled water for 20min and steam sterilized. Tube length was 12cm except for experiments with stents, which used 4cm-long tubes to reduce background signal from undisturbed cells in unstented parts of the tube. Tubes were coated with 100µg/ml fibronectin (Sigma) in PBS for 2h, while rotating at 10rph at 37°C (Figure 1A) and rinsed to remove loosely adsorbed fibronectin. Homotypic constructs were fabricated with injection of EC or SMC into fibronectin-coated tubes ($8 \cdot 10^5$ cells/ml), and cultured for 24h at 37°C, under

axial rotation. Sequential layering of SMC, followed by application of EC produced SMC/EC vessel-like constructs. SMC were seeded on fibronectin-coated tubes ($8 \cdot 10^5$ cells/ml), forming a SMC multi-layer (Figure 1B, 1E). After 24h adhesion under axial rotation constructs were filled with an EC suspension ($8 \cdot 10^5$ cells/ml) and incubated for 24h. Cells within constructs were characterized for constitutive and inducible markers and biosecretory function (Table 1S). Appropriate cell assembly within constructs was verified by confocal microscopy and cell coverage quantified using MATLAB[®]-based image analysis programs (Video 1S).

The SMC/EC vessel-like constructs were connected to 60cm-long loops of Silastic[®] tubing containing fresh EC complete medium and rested for 24h to ensure complete 'endothelialization' (Figure 1C, 1F). Supplemented medium was replaced by EBM-2 medium to starve the cells overnight prior to perfusion. Cell-seeded constructs were placed in a perfusion bioreactor^{18, 19} and exposed to controlled coronary artery-like flow -1Hz pulsatile flow of 17 dyn/cm^2 average shear stress. In all experiments, samples without flow served as controls. In experiments with growth factors (GF), EC and SMC complete media was used for EC and SMC homotypic constructs, respectively, while SMC/EC vessel-like constructs were perfused with EC complete medium.

Injury model

EC-only and SMC/EC vessel-like constructs were stented with 7-cell stainless steel NIR stents ($3.5 \times 16 \text{ mm}$, Medinol). To discriminate direct drug-mediated effect from flow-mediated modulation of drug treatment, 1h before stent implantation 10nM temsirolimus (Wyeth) was added to the starvation media. This dose abrogates mTOR signaling in endothelial cells²⁰. DMSO at the doses used has no effect on mTOR activation status²⁰.

Measurement of p-S6RP expression by flow cytometry

We used our perfusion bioreactor and the vessel-like constructs to examine mTOR signaling in cells exposed to coronary-like flow. mTOR activation status was assessed measuring phosphorylation levels of S6 ribosomal protein (S6RP), a downstream substrate of TORC1. Phospho-S6RP (p-S6RP) is a more reliable index in our experiments, as total mTOR may be conserved even in the face of shunting to the TORC1 or TORC2 protein complexes. EC in SMC/EC co-cultures were identified with PE-conjugated anti-CD31 antibody (BD Pharmingen). Double staining of EC with this antibody and FITC-conjugated anti-p-S6RP allowed for cell and signal co-localization. Levels of p-S6RP were measured at 'basal' conditions, and following flow exposure, stent placement and incubation with temsirolimus. Cells were recovered from constructs by 3min-trypsin treatment, washed and resuspended in Fixation/Permeabilization Buffer Solution (BD Biosciences) for 30min. Trypsin had no impact on CD31 cytometric detection in EC. After detachment, samples were rinsed twice with 10% Fixation Buffer (BD Biosciences) in PBS and incubated in suspension with FITC-conjugated anti-p-S6RP (Cell Signaling) or appropriate isotypic control for 30min at 4°C. Cells were analyzed by flow cytometry using a FACS calibur instrument and Cell Quest software (Becton Dickinson). Positive cells were gated to determine respective mean intensity fluorescence (MIF) (Figure 2C), background autofluorescence from unlabeled cells was subtracted, and data presented as the quotient of MIF of samples exposed to flow and corresponding static controls.

RIPA and digitonin extraction

Non-specific cell lysis was performed by rinsing cell-coated constructs twice with ice cold PBS and then incubating them for 30min on ice in RIPA buffer containing 50mM Tris-HCl, pH 7.4, 150mM NaCl, 1% NP-40, 0.5% sodium deoxycholate, 0.1% SDS and 5mM EDTA. The supernatant was obtained after centrifugation for 30min at 4°C. Specific cytosolic extraction of surface cells on the constructs was achieved with digitonin. Cells washed with

ice-cold PBS were covered with buffer containing 120mM KCl, 5mM KH₂PO₄, 10mM HEPES, pH 7.4, 2mM EGTA, 0.15mg/ml digitonin (Sigma) and rocked gently on ice for 30min. The gently-aspirated supernatant was labeled as digitonin extract^{21, 22}. Absence of SMC in the extracts was verified by blotting membranes against anti-SMC α -actin and anti-tubulin antibodies (Sigma) (Figure 2S. A).

Western Blot analysis

10% acrylamide gels (Invitrogen) were used for protein separation. Gels were blotted using Invitrogen gel transfer stacks and blotting system. Membranes were blocked with 5% powdered milk and incubated overnight with primary monoclonal anti-p-S6RP (Cell Signaling, 1:1,000 dilution) and anti- β actin (Santa Cruz Biotech, 1:15,000 dilution) at 4°C while shaking. After two washes with PBS-T (PBS, 0.05% Tween20), membranes were incubated with HRP-conjugated secondary antibodies (Santa Cruz Biotech, 1:3,500 dilution) for 2h while shaking at room temperature. After two 10min washes in PBS-T, Supersignal West Femto Maximum Sensitivity substrate (Pierce) was applied and luminescence detected in an Alpha Innotec FluorChem. Densitometry plots were analyzed using ImageJ.

Microscopic examinations

Endothelial monolayer integrity within constructs was assessed using fluorescence (Perkin-Elmer spinning disk confocal system coupled to a Zeiss Axiovert 200M microscope) and scanning electron microscopy (SEM)(Figure 1). Constructs, embedded in a protective outer tubular layer prior to removal from the loops to minimize stress and artifactual effects on the cellular lining, were rinsed with PBS, and fixed with 4% paraformaldehyde (Mallinckrodt) for 20min at room temperature. After two consecutive washes with PBS for 10min and 1h blotting with 5% goat serum in PBS-BSA (PBS, 1% bovine serum albumin), EC and SMC were labeled for 1h with rabbit monoclonal anti-CD31 (Abcam) and mouse anti-Tissue Factor (American Diagnostica) diluted 1:50 in PBS-BSA. Cells were rinsed twice with PBS-BSA for 10min and stained with goat anti-rabbit Alexa Fluor[®] 488 and goat anti-mouse Alexa Fluor[®] 647 (1:100 in PBS-BSA) secondary antibodies and DAPI solution (1:500 in PBS-BSA) for 1h. Two 10min washes with PBS were performed to remove any unbound antibody. Vessels were longitudinally sectioned with a surgical blade for imaging. To image stents within constructs (Figure 1G), stents were removed from the longitudinally sectioned constructs and cut open using surgical scissors. When imaging p-S6RP expression (Figure 1S), fixed cells were permeabilized with 0.2% triton in PBS for 10 min. Cells were washed with PBS twice for 10min, blotted and stained with rabbit monoclonal antibody against p-S6RP (Cell Signaling, 1:50 dilution in PBS-BSA) and the corresponding Alexa Fluor[®] 488 conjugated secondary antibody (1:100 in PBS-BSA).

For SEM, stents were removed from the cell-coated constructs and stent struts imaged directly using low vacuum EI/Philips XL30 FEG environmental SEM (Figure 1D). Cells on constructs were fixed in 4% paraformaldehyde, rinsed with PBS and subject to serial dehydration, with 30min-incubations in solutions of increasing ethanol content (50, 70, 95, 100%) and 1h in acetone. Specimens were air-dried overnight, sputter coated for 45s using a Denton Vacuum Desk II Sputter Coater and imaged with a Hitachi S-3400N SEM.

In vivo studies

The left anterior descending coronary and right coronary arteries of Yucatan pigs were implanted with 6 cell, 3×13mm bare metal (Neo Stent, Co/Cr alloy) or sirolimus-eluting (Neo Stents coated with 50/50(w/w) PEVA and PBMA containing 120 μ g sirolimus, JnJ/Cordis) stents. Animal care and procedures followed AAALAC and NIH guidelines. On the 7th (n=3) and 30th day (n=8) post-stenting, animals were terminally anesthetized with pentobarbital (65 mg/kg). After sacrifice, stented vessels were dissected free, and pressure perfused with PBS

followed by 10% formalin. After ethanol and xylene processing, vessels were embedded whole in a methyl methacrylate/butyl methacrylate resin (Polysciences Inc.) and polymerized under UV light. Serial cross-sectional planes were obtained along the length of the stents with a precision saw, microtome-cut at 5 μ m-thickness and stained with verHoeff's elastin and H&E stains and for specific cell markers (CD31, α -actin, p-S6RP)(Supplemental Figure 3). Unstented coronary segments were embedded in paraffin. Rabbit anti-p-S6RP monoclonal antibody (Cell Signaling) with low-temperature antigen retrieval and a tyramide signal amplification system (DakoCytomation) was used for immunohistochemical analysis of mTOR. Quantitative morphometric analysis was performed on the histological sections from each stented artery.

Statistics

In all figures, data are expressed as average \pm standard deviation. Non parametric Kruskal Wallis test followed by Scheffe post hoc analysis of the original measured values normalized to their corresponding controls were conducted to determine statistical differences between values; p values <0.05 were considered significant.

RESULTS

Basal mTOR/TORC1 signaling is modulated by flow in EC but not in SMC

Though endothelial and smooth muscle cells rendered quiescent by GF deprivation exhibited low levels of p-S6RP, they also showed differential responses to flow and GF. EC expression of p-S6RP nearly doubled within 20min exposure to coronary-like flow (1Hz pulsatile, 17dyn/cm²) (1.97 \pm 0.2 fold increase; p<0.5; Figure 2A). A 1.96 \pm 0.4-fold increase in p-S6RP upregulation was confirmed by immunoblotting using Western blotting after whole cell lysis and with digitonin extraction (Figure 3C, Figure 2S. B). Confocal imaging of adherent EC revealed 1.91 \pm 0.2 upregulation of S6RP phosphorylation under flow (Figure 3E, Figure 1S). Growth factor exposure had no significant effect on S6RP phosphorylation in EC (Figure 2A). In contrast SMC were unaffected by flow but exhibited almost five-fold increase in p-S6RP expression upon GF exposure (p < 0.05 vs. static control; Figure 2B). Thus, mTOR/TORC1 signaling in EC is most sensitive to alterations in shear stress; while the local biochemical milieu dominates in SMC. Homotypic studies were augmented by SMC/EC vessel-like constructs. Interestingly, the presence of SMC reduced flow-induced S6RP phosphorylation in EC (MIF flow/static 1.16 \pm 0.04 vs. 1.97 \pm 0.2 in EC-only vessel-like constructs; p<0.05; Figure 2D, Figure 2S.C) and EC eliminated the GF responsiveness of SMC p-S6RP expression (Figure 2E).

Differential effect of flow and static regimens on p-S6RP status in EC following stent-induced injury

Under static conditions p-S6RP expression in EC lining conduits rose with stent injury (1.32 \pm 0.1 fold), but not when SMC were present as well (0.90 \pm 0.2-fold, p<0.05). Interestingly, the expected flow-mediated increase in p-S6RP expression seen in quiescent, monolayered EC was lost in EC injured by stent placement (0.91 \pm 0.1, p<0.05 compared to static) and reduced when EC were in SMC/EC vessel-like constructs (0.77 \pm 0.1, p<0.05 compared to static).

mTOR blockade by Temsirolimus eliminates *in vitro* flow and growth factor-induced mTOR/TORC1 activation, and delays post-stenting re-endothelialization

Sirolimus/FKBP12 complexes interact specifically with mTOR/TORC1, blocking downstream targets, S6K1 and its substrate S6RP. Temsirolimus reduced flow and GF-induced p-S6RP levels in EC and SMC (Figure 3). mTOR blockade markedly affected re-endothelialization post-stenting. The number of CD31 positive cells on the luminal surface of

stents struts after 24h flow exposure was 3.5 ± 0.4 -fold* reduced by temsirolimus constructs with EC alone and by 2.2 ± 0.4 -fold* with SMC present as well (* $p < 0.05$) (Figure 4S). These results confirm that temsirolimus is a powerful blocker of the mTOR machinery and suggest that its effects are more profound when expression of S6RP is highest as in EC without underlying SMC.

Immunohistochemical analysis of p-S6RP expression was performed in coronary arteries stented with sirolimus-eluting stents or control BMS. Endothelialization was not significantly different in the different stent arteries (3.1 ± 0.2 vs 2.3 ± 0.50). Specific p-S6RP staining was identified in the endothelium and some leukocytes (macrophages and lymphocytes) in the neointima of the 7-day BMS but no cells stained in the 7-day sirolimus-eluting stent (Figure 4A and 4B). Control unstented arteries did not show any cells expressing p-S6RP (Figure 4C). More importantly, quantitative analysis of the luminal surface of the bare metal stented vessels revealed that the highest percentage of p-S6RP positive cells at the neointima luminal surface (Figure 4D and 4E). Phospho-S6RP is upregulated in the neointima of BM-stented arteries; phosphorylation inversely correlates with the presence of underlying SMC. These findings provide *in vivo* evidence that healthy EC do not express p-S6RP. Conversely, injured EC do express p-S6RP and the expression is sensitive to their surrounding milieu -fibrin and inflammatory cells in the neointima vs SMC in the media (Figure 3S). The ability, however, of EC to restore the balance after intervention is lost in the presence of mTOR inhibitors.

DISCUSSION

The S6/mTOR pathway is critical for vascular reactivity and metabolism. We now show that phosphorylation of S6 ribosomal protein in EC is flow-sensitive, and in SMC GF-mediated. We also demonstrate that the response of the intact vessel cannot be appreciated by examining isolated vascular cells. Using a custom designed flow system that allowed for coating of loop conduits with EC alone or EC on layers of SMC we demonstrated how EC S6RP signaling is mediated by adjacent SMC and vice versa. SMC inhibit flow-mediated mTOR activation in EC and reciprocally EC regulated the response in SMC. Cell-seeded perfusion systems allow examination of specific cellular elements under defined flow and shear conditions, with exposure to specific concentrations of vasoregulators, and over a short time scale without tissue remodeling. Our vessel-like constructs extend similar systems²³⁻³⁰ by introducing a bilayer co-culture of EC and SMC within tubular structures that enable microscopic examination, programmed chemical and mechanical intervention, correlation of intracellular signaling events with functional outcome, and under static or coronary artery-like flow¹⁸. The use of cells and defined media is here superior to excised vessels and whole blood as we can associate particular signals with specific cells under precisely controlled flows. Digitonin extraction enables determination of S6RP phosphorylation in EC even in culture with SMC. At low concentrations digitonin, a gentle detergent, selectively punctures 8-10 nm holes in the sterol-rich plasma membrane, allowing leakage of cytosolic proteins of up to 200 kDa mass. Moreover, digitonin exerts effect only in cells it directly contacts^{21, 22}. Digitonin-extracted SMC/EC vessel-like constructs revealed S6RP phosphorylation without effects on SMC as there was no significant release of SMC α -actin (Figure 2S.A).

The trilaminar architecture of the blood vessel provides structural support and a platform from which to launch an array of intricate paracrine regulation – primary among which are the interactions between EC and SMC. Each cell can induce phenotypic transformations and different bioregulatory states in the other^{31,32}. EC spread slower and present a less thrombotic phenotype when cultured on SMC^{33, 34}. Similarly, the EC pro-coagulant and pro-inflammatory phenotype is amplified in co-culture with growth factor-stimulated SMC and subdued in co-culture with growth factor-deprived SMC³⁵. EC modulate the contractile and growth properties of vascular SMC in turn³⁶⁻³⁹. Our results on flow- and GF-mediated activation of S6RP provide

further evidence of EC-SMC cross talk. In health, EC are exposed to flow and SMC are buffered from blood by the endothelial monolayer. With injury, the endothelium is disturbed and SMC are now directly exposed to flow. Classic studies cite these events as critical to mediation of vasomotor tone⁴⁰⁻⁴². This view of vascular cell architecture relative to flow perhaps best explains why flow upregulates p-S6RP in EC and GF upregulate this path way in SMC. What is fascinating is that this upregulation is observed only for cells in isolation, co-cultured cells are far more quiescent. That SMC-EC co-regulation extends to p-S6RP is doubly intriguing. The mTOR pathway is a primary metabolic sensor of the cell. SMC might induce metabolic activity within EC via a paracrine mechanism or direct cell-cell contact.

Differential expression of proteins within them TOR signaling pathway has profound implications. Local injury, flow and chemical inhibition synergize to disrupt the endothelial monolayer, prevent its restoration and impair its function. Interactions between EC and SMC are more important in regulating vascular wall hemostasis than previously anticipated; both EC and SMC alter the expression of factors in coagulation and fibrinolysis in response to shear stress⁴³. Shyy and co-workers observed that while laminar shear stress activated AMPK and Akt in EC, disturbed flow activated only Akt⁴⁴, disrupting the balance of mTOR and S6K; increasing the proportion of EC in a mitotic state. Our two-fold upregulation of mTOR in EC by flow is in direct concert with these studies and has now been expanded to SMC as well. Our results indicate that in vessel-like constructs EC-SMC interaction dominates, altering the dynamics of basal mTOR signaling and overriding GF pro-angiogenic stimulation. Such results take us back to Virchow on the one hand and bring us to the present day of DES and their attendant potential complications on the other. Similar to the triad of Virchow that governs venous thrombosis we observe that signaling within EC and SMC resident in the vessel wall are set by the biochemical milieu established by blood, local flow disruptions and the state of the wall and its cells. The relative effects of the stent itself on the EC and SMC may explain the enhanced sensitivity of the endothelium after local delivery of agents that interfere with mTOR signaling. Endothelial denudation is most prominent between the stent struts at the time of implantation, and most rapidly recovers in this region perhaps because these EC regenerate over SMC and can more quickly attain a mature endothelial phenotype. EC over the stent struts do not readily regain this mature, confluent and bioregulatory phenotype and retain p-S6RP expression even when physically contiguous because they are distant from SMC. One might then explain strut-adherent thrombosis in DES with incomplete endothelial healing as evidenced by persistent p-S6RP expression.

The modified triad, inflammation from the foreign materials of the stent, toxic effects of the pooled drug, and flow disruptions from the strut, might all contribute to but cannot account alone for the repair *in vivo*. *In vitro* stenting results may be masked by surrounding uninjured EC present in the flow cytometric analysis. Thus, despite the complimentary findings that EC-SMC interactions affect EC phosphorylation of S6RP in response to stent injury *in vivo* and *in vitro*, the levels of S6RP phosphorylation after stenting in our *in vitro* system lacked the spatial resolution needed to directly compare them to the *in vivo* state. Contact-mediated SMC regulation of EC signaling needs to be defined further and confirmed, but may allow better understanding of the vascular response to DES and how drugs that have one putative mode of activity when examined in isolated cultures can behave in unanticipated manners in the intact and injured *in vivo* system. It is important to remember that stents are placed in disease arteries, with complex bifurcated geometries, blood enriched perhaps in LDL, glucose and a number of prescription drugs, and a plaque. All of those elements will definitively alter the interactions between EC and SMC.

That S6RP phosphorylation was flow-sensitive in EC and GF-sensitive in mural SMC and that SMC dominate over EC has important fundamental and clinical implications. Investigation of the basic signaling should now consider the cells alone and together, and use of DES must

integrate stent design influence on flow and drug impact on mTOR. The use of flow models, flow activated cell sorting, intracellular signaling in a co-culture of human vascular cells and modern clinical interventions can provide new insight into fundamental biology. Our flow system can track mTOR and up-and downstream signaling molecules at rest, under flow and with exposure to drugs over a span of concentrations and delivery kinetics. Novel endoscopic confocal microscopes will allow us to relate flow alterations with cell function and drug localization. Stents are placed in diseased arteries, with thickened diseased walls, in the presence of clot and inflammation, a complex and potentially disarrayed matrix of endothelial and smooth muscle cells, complex bifurcated geometries, and blood enriched with lipoproteins, glucose and possibly drugs, that may be subject to altered flow. All of those elements will affect the interactions between EC and SMC, and all must be considered in appreciating vascular cell communication and homeostasis, but few of them can be reproduced in a consistent and independent fashion. Flow models with multiple cell systems under defined flow regimes bring us back to Virchow and forward into the era of complex vascular interventions and emerging concepts in vascular biology.

Supplementary Material

Refer to Web version on PubMed Central for supplementary material.

Acknowledgments

The authors thank Philip Seifert for his support in IHC, Sylaja Murikipudi and Laith Rabadi for their support in WB analysis, Dr. Yoram Richter (Medinol) for the gift of NIR stents and Wyeth Laboratories for the temsirolimus. We thank Cordis Corp. for providing access to specimens used to obtain preclinical *in vivo* data.

FUNDING SOURCES

NIH/NIGMS RO1/GM049039 (E. Edelman). NIH-NIDDK (1K08DK080946) (V. Chitalia). M. Balcells is supported by the Barcelona Chamber of Commerce, and Fundació Empreses IQS.

ABBREVIATION LIST

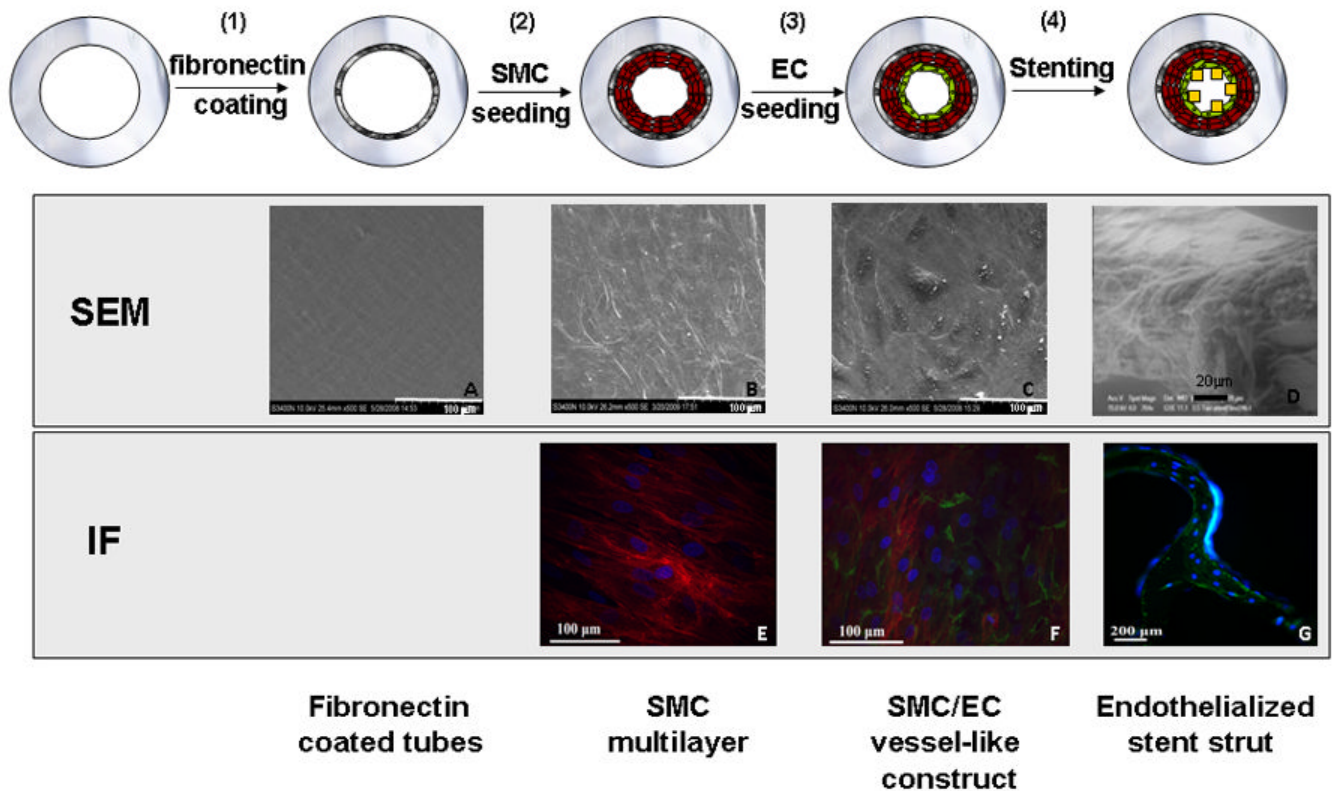
EC	Endothelial cells
SMC	Smooth muscle cells
DES	Drug eluting stent
BMS	Bare metal stent
mTOR	Mammalian target of rapamycin
p-S6RP	Phosphorylated S6 ribosomal protein
SEM	Scanning electron microscopy
FACS	Fluorescence activated cell sorting
IF	Immunofluorescence
MIF	Mean intensity fluorescence
Tems	Temsirolimus (mTOR inhibitor)
BSA	Bovine serum albumin
PBS	Phosphate buffer saline

References

1. Joner M, Finn AV, Farb A, Mont EK, Kolodgie FD, Ladich E, Kutys R, Skorija K, Gold HK, Virmani R. Pathology of drug-eluting stents in humans: delayed healing and late thrombotic risk. *J Am Coll Cardiol* 2006;48:193–202. [PubMed: 16814667]
2. Serruys PW, Kukreja N. Late stent thrombosis in drug-eluting stents: return of the ‘VB syndrome’. *Nat Clin Pract Cardiovasc Med* 2006;3:637. [PubMed: 17122790]
3. Steffel J, Latini RA, Akhmedov A, Zimmermann D, Zimmerling P, Luscher TF, Tanner FC. Rapamycin, but not FK-506, increases endothelial tissue factor expression: implications for drug-eluting stent design. *Circulation* 2005;112:2002–2011. [PubMed: 16172265]
4. Camici GG, Steffel J, Amanovic I, Breitenstein A, Baldinger J, Keller S, Luscher TF, Tanner FC. Rapamycin promotes arterial thrombosis in vivo: implications for everolimus and zotarolimus eluting stents. *Eur Heart J* 2010;31:236–242. [PubMed: 19567381]
5. Smith EJ, Jain AK, Rothman MT. New developments in coronary stent technology. *J Interv Cardiol* 2006;19:493–499. [PubMed: 17107363]
6. Jiang BH, Liu LZ. Role of mTOR in anticancer drug resistance: perspectives for improved drug treatment. *Drug Resist Updat* 2008;11:63–76. [PubMed: 18440854]
7. Zeng Z, Sarbassov dos D, Samudio IJ, Yee KW, Munsell MF, Ellen Jackson C, Giles FJ, Sabatini DM, Andreeff M, Konopleva M. Rapamycin derivatives reduce mTORC2 signaling and inhibit AKT activation in AML. *Blood* 2007;109:3509–3512. [PubMed: 17179228]
8. Sarbassov DD, Ali SM, Sengupta S, Sheen JH, Hsu PP, Bagley AF, Markhard AL, Sabatini DM. Prolonged rapamycin treatment inhibits mTORC2 assembly and Akt/PKB. *Mol Cell* 2006;22:159–168. [PubMed: 16603397]
9. Kolachalama VB, Tzafirri AR, Arifin DY, Edelman ER. Luminal flow patterns dictate arterial drug deposition in stent-based delivery. *J Control Release* 2009;133:24–30. [PubMed: 18926864]
10. Balakrishnan B, Dooley J, Kopia G, Edelman ER. Thrombus causes fluctuations in arterial drug delivery from intravascular stents. *J Control Release* 2008;131:173–180. [PubMed: 18713645]
11. Balakrishnan B, Dooley JF, Kopia G, Edelman ER. Intravascular drug release kinetics dictate arterial drug deposition, retention, and distribution. *J Control Release* 2007;123:100–108. [PubMed: 17868948]
12. Balakrishnan B, Tzafirri AR, Seifert P, Groothuis A, Rogers C, Edelman ER. Strut position, blood flow, and drug deposition: implications for single and overlapping drug-eluting stents. *Circulation* 2005;111:2958–2965. [PubMed: 15927969]
13. Miyauchi K, Kasai T, Yokoyama T, Aihara K, Kurata T, Kajimoto K, Okazaki S, Ishiyama H, Daida H. Effectiveness of statin-eluting stent on early inflammatory response and neointimal thickness in a porcine coronary model. *Circ J* 2008;72:832–838. [PubMed: 18441467]
14. Baker AB, Groothuis A, Jonas M, Etnenson DS, Shazly T, Zcharia E, Vlodaysky I, Seifert P, Edelman ER. Heparanase alters arterial structure, mechanics, and repair following endovascular stenting in mice. *Circ Res* 2009;104:380–387. [PubMed: 19096032]
15. Jonas M, Edelman ER, Groothuis A, Baker AB, Seifert P, Rogers C. Vascular neointimal formation and signaling pathway activation in response to stent injury in insulin-resistant and diabetic animals. *Circ Res* 2005;97:725–733. [PubMed: 16123336]
16. Blackman BR, Garcia-Cardena G, Gimbrone MA Jr. A new in vitro model to evaluate differential responses of endothelial cells to simulated arterial shear stress waveforms. *J Biomech Eng* 2002;124:397–407. [PubMed: 12188206]
17. Garcia-Cardena G, Gimbrone MA Jr. Biomechanical modulation of endothelial phenotype: implications for health and disease. *Handb Exp Pharmacol* 2006:79–95. [PubMed: 16999225]
18. Balcells M, Fernandez Suarez M, Vazquez M, Edelman ER. Cells in fluidic environments are sensitive to flow frequency. *J Cell Physiol* 2005;204:329–335. [PubMed: 15700266]
19. Methe H, Balcells M, Alegret Mdel C, Santacana M, Molins B, Hamik A, Jain MK, Edelman ER. Vascular bed origin dictates flow pattern regulation of endothelial adhesion molecule expression. *Am J Physiol Heart Circ Physiol* 2007;292:H2167–2175. [PubMed: 17209004]

20. Costa LF, Balcells M, Edelman ER, Nadler LM, Cardoso AA. Proangiogenic stimulation of bone marrow endothelium engages mTOR and is inhibited by simultaneous blockade of mTOR and NF-kappaB. *Blood* 2006;107:285–292. [PubMed: 16141350]
21. Chitalia VC, Foy RL, Bachschmid MM, Zeng L, Panchenko MV, Zhou MI, Bharti A, Seldin DC, Lecker SH, Dominguez I, Cohen HT. Jade-1 inhibits Wnt signalling by ubiquitylating beta-catenin and mediates Wnt pathway inhibition by pVHL. *Nat Cell Biol* 2008;10:1208–1216. [PubMed: 18806787]
22. Schulz I. Permeabilizing cells: some methods and applications for the study of intracellular processes. *Methods Enzymol* 1990;192:280–300. [PubMed: 2074793]
23. Niwa K, Kado T, Sakai J, Karino T. The effects of a shear flow on the uptake of LDL and acetylated LDL by an EC monoculture and an EC-SMC coculture. *Ann Biomed Eng* 2004;32(4):537–543. [PubMed: 15117027]
24. Wada Y, Sugiyama A, Kohro T, Kobayashi M, Takeya M, Naito M, Kodama T. In vitro model of atherosclerosis using coculture of arterial wall cells and macrophage. *Yonsei Med J* 2000;41:740–755. [PubMed: 11204825]
25. Chiu JJ, Chen LJ, Lee PL, Lee CI, Lo LW, Usami S, Chien S. Shear stress inhibits adhesion molecule expression in vascular endothelial cells induced by coculture with smooth muscle cells. *Blood* 2003;101:2667–2674. [PubMed: 12468429]
26. Chiu JJ, Chen LJ, Chen CN, Lee PL, Lee CI. A model for studying the effect of shear stress on interactions between vascular endothelial cells and smooth muscle cells. *J Biomech* 2004;37:531–539. [PubMed: 14996565]
27. Fillinger MF, Sampson LN, Cronenwett JL, Powell RJ, Wagner RJ. Coculture of endothelial cells and smooth muscle cells in bilayer and conditioned media models. *J Surg Res* 1997;67:169–178. [PubMed: 9073564]
28. Nackman GB, Bech FR, Fillinger MF, Wagner RJ, Cronenwett JL. Endothelial cells modulate smooth muscle cell morphology by inhibition of transforming growth factor-beta 1 activation. *Surgery* 1996;120:418–425. discussion 425–416. [PubMed: 8751613]
29. Jacot JG, Wong JY. Endothelial Injury Induces Vascular Smooth Muscle Cell Proliferation in Highly Localized Regions of a Direct Contact Co-culture System. *Cell Biochem Biophys* 2008;52:37–46. [PubMed: 18766304]
30. Gong Z, Niklason LE. Blood vessels engineered from human cells. *Trends Cardiovasc Med* 2006;16:153–156. [PubMed: 16781948]
31. Xu S, He Y, Vokurkova M, Touyz RM. Endothelial cells negatively modulate reactive oxygen species generation in vascular smooth muscle cells: role of thioredoxin. *Hypertension* 2009;54:427–433. [PubMed: 19564543]
32. Wang YH, Yan ZQ, Shen BR, Zhang L, Zhang P, Jiang ZL. Vascular smooth muscle cells promote endothelial cell adhesion via microtubule dynamics and activation of paxillin and the extracellular signal-regulated kinase (ERK) pathway in a co-culture system. *Eur J Cell Biol* 2009;88:701–709. [PubMed: 19581021]
33. Wallace CS, Strike SA, Truskey GA. Smooth muscle cell rigidity and extracellular matrix organization influence endothelial cell spreading and adhesion formation in coculture. *Am J Physiol Heart Circ Physiol* 2007;293:H1978–1986. [PubMed: 17644568]
34. Imberti B, Seliktar D, Nerem RM, Remuzzi A. The response of endothelial cells to fluid shear stress using a co-culture model of the arterial wall. *Endothelium* 2002;9:11–23. [PubMed: 12901357]
35. Rose SL, Babensee JE. Smooth muscle cell phenotype alters cocultured endothelial cell response to biomaterial-pretreated leukocytes. *J Biomed Mater Res A* 2008;84:661–671. [PubMed: 17635014]
36. Mosse PR, Campbell GR, Campbell JH. Smooth muscle phenotypic expression in human carotid arteries. II. Atherosclerosis-free diffuse intimal thickenings compared with the media. *Arteriosclerosis* 1986;6:664–669. [PubMed: 3778309]
37. Herman IM, Castellet JJ Jr. Regulation of vascular smooth muscle cell growth by endothelial-synthesized extracellular matrices. *Arteriosclerosis* 1987;7:463–469. [PubMed: 3675305]
38. Sabatini PJ, Zhang M, Silverman-Gavrila R, Bendeck MP, Langille BL. Homotypic and endothelial cell adhesions via N-cadherin determine polarity and regulate migration of vascular smooth muscle cells. *Circ Res* 2008;103:405–412. [PubMed: 18617695]

39. Mack PJ, Zhang Y, Chung S, Vickerman V, Kamm RD, Garcia-Cardena G. Biomechanical regulation of endothelial-dependent events critical for adaptive remodeling. *J Biol Chem* 2009;284:8421–8420. [PubMed: 19189966]
40. Feletou M, Vanhoutte PM. Endothelium-derived hyperpolarizing factor: where are we now? *Arterioscler Thromb Vasc Biol* 2006;26:1215–1225. [PubMed: 16543495]
41. Furchgott RF. Nitric oxide: from basic research on isolated blood vessels to clinical relevance in diabetes. *An R Acad Nac Med (Madr)* 1998;115:317–331. [PubMed: 9882827]
42. Furchgott RF. Endothelium-derived relaxing factor: discovery, early studies, and identification as nitric oxide. *Biosci Rep* 1999;19:235–251. [PubMed: 10589989]
43. Helenius G, Hagvall SH, Esguerra M, Fink H, Soderberg R, Risberg B. Effect of shear stress on the expression of coagulation and fibrinolytic factors in both smooth muscle and endothelial cells in a co-culture model. *Eur Surg Res* 2008;40:325–332. [PubMed: 18303268]
44. Guo D, Chien S, Shyy JY. Regulation of endothelial cell cycle by laminar versus oscillatory flow: distinct modes of interactions of AMP-activated protein kinase and Akt pathways. *Circ Res* 2007;100:564–571. [PubMed: 17272808]



CIRCULATIONAHA/2009/877282

Figure 1. Layer-by-layer assembly and intervention of a vessel-like construct

In vitro model of stent-induced vascular injury. EC alone or with SMC were layered onto the inner surface of fibronectin coated silicon-rubber tubes and left intact or stented. Luminal construct morphology at each stage was obtained by SEM. The cobblestone morphology typical of EC on naïve vessels and *in vitro* cultures can be observed in the undisturbed SMC/EC vessel-like constructs (C) but is lost on the stent strut surface (D). Immunofluorescence imaging identified specific cells -EC (in green) are labeled using anti-CD31 monoclonal antibody conjugated to an AlexaFluor® 488 secondary antibody. SMC (in red) are labeled using anti-Tissue Factor monoclonal antibody conjugated to an AlexaFluor® 647 secondary antibody. Each assembly step was imaged in three different experiments, each including three independent constructs. All constructs were divided into 4–6 sections that were scanned and photographed 8–10 times.

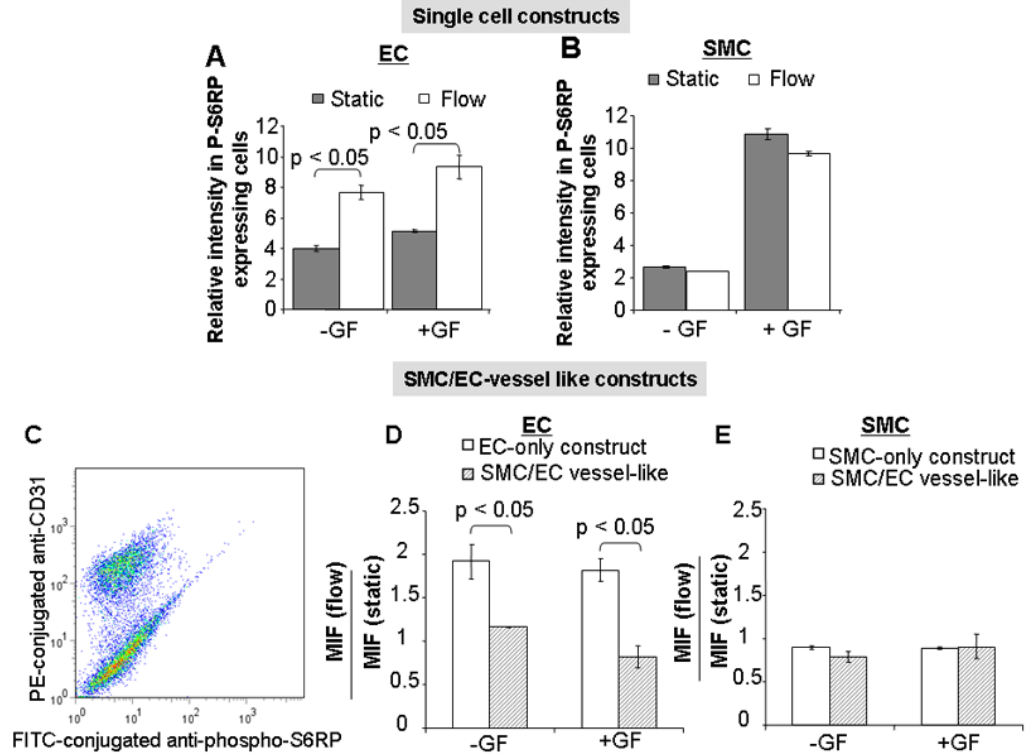


Figure 2. Impact of flow and growth factors on p-S6RP expression

While coronary artery-like flow upregulated p-S6RP expression in EC, but not in SMC, growth factor stimulation induced S6RP phosphorylation in SMC but not EC (A, B). **SMC regulate EC response to flow. EC dictate SMC response to growth factors.** C) Representative flow-cytometric separation of SMC and EC in SMC/EC vessel-like constructs. After detachment from tubes, p-S6RP expression in both cell types was quantified with a FITC-conjugated anti-p-S6RP antibody. EC in the EC/SMC mixture were specifically stained with PE-conjugated CD31 antibody. When EC were seeded on a SMC multilayer, EC S-6RP phosphorylation became flow-independent (D). S-6RP phosphorylation was independent of flow in SMC, both when SMC were alone or when shielded by overlying EC (E). All figure bars represent the average of twelve data points \pm SD obtained in three experiments that included four independent observations of each conditioned assayed.

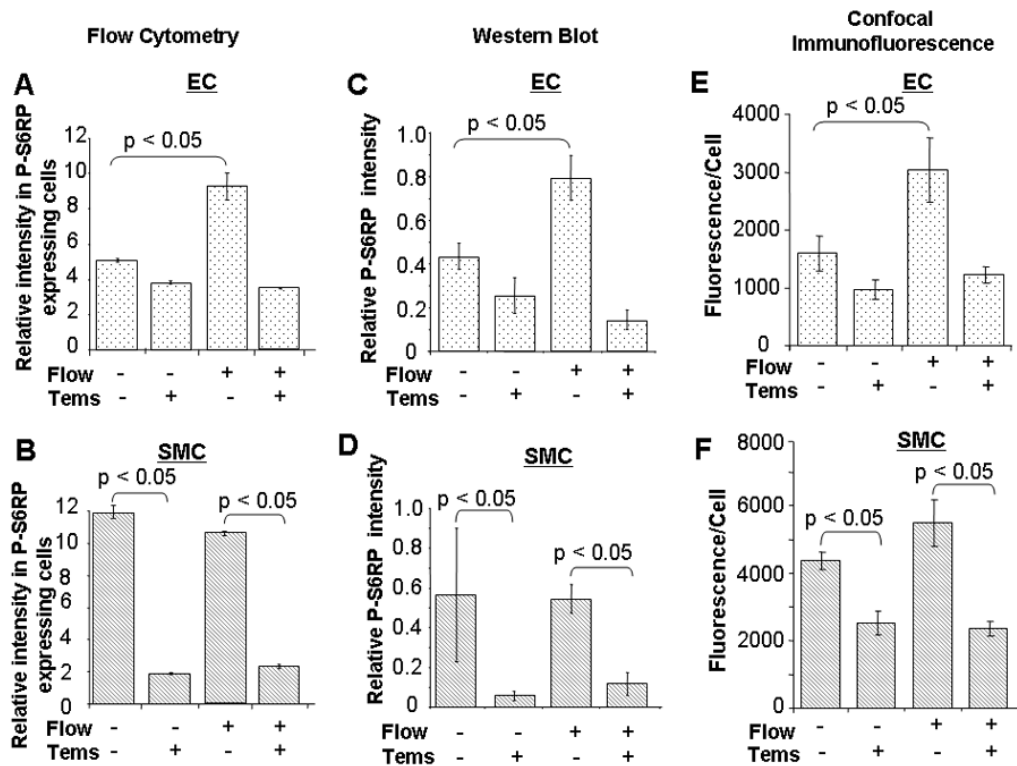


Figure 3. Tamsirolimus effectively blocks the mTOR pathway

The flow and tamsirolimus response of isolated EC and SMC obtained by FACS (A, B) were confirmed by protein expression by Western blots (C, D) and under confocal immunofluorescence (E, F). n=12 (three experiments, four independent observations of each condition assayed).

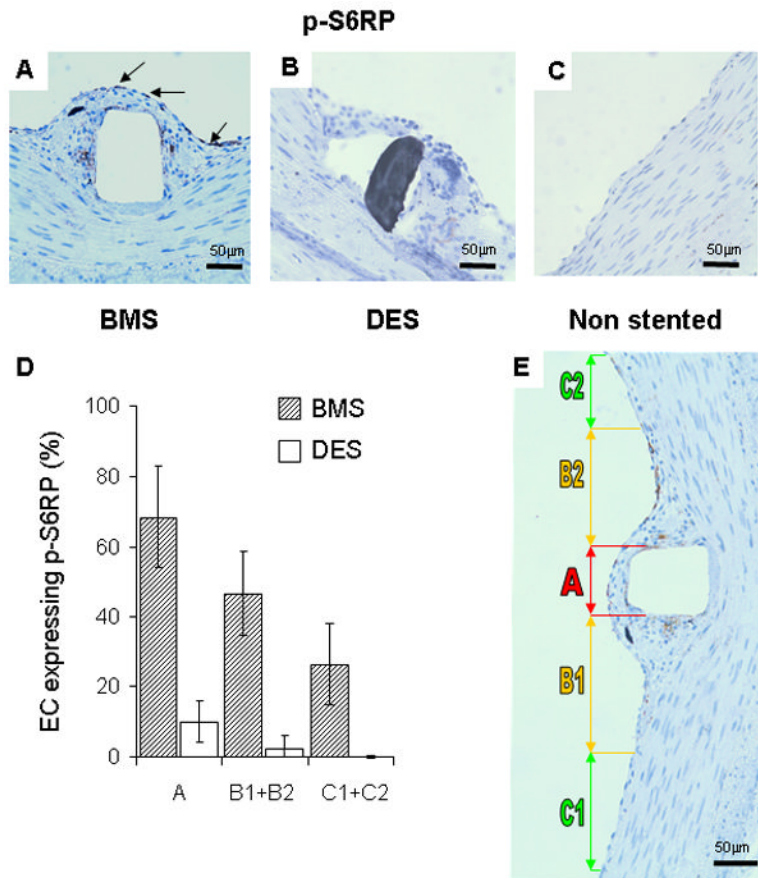


Figure 4. Injury and sirolimus alter p-S6RP expression in EC. The highest degree of S6RP phosphorylation *in vivo* occurs where EC are farthest from intact SMC

(A) p-S6RP expression was prominent in extracted porcine coronary arteries stented with BMS (arrows indicate positive staining cells in brown) and eliminated in sirolimus-eluting stents (B). Unstented control arteries (C) had an intact endothelium and media with no detectable p-S6RP staining. The incidence of p-S6RP positive EC in the luminal surface correlated with the nature of the underlying layer (D) and plotted by region relative to the stent strut (E). Region A is directly above the stent strut, B1 and B2 correspond to areas within the neointima adjacent to the stent strut, and C1 and C2 are regions where there is healthy endothelium, no detectable neointima and viable SMC within a normal medial layer (E). Only at a distance from the stent strut beyond the neointima/intact media boundary (zones C1 and C2) was the number of p-S6RP positive EC significantly reduced. n=12 (three experiments, four independent observations each).